Replacement-Free Electrodeless QCM Using Nonspecific-Adsorption of Streptavidin on Quartz

Journal:	*Analytical Chemistry*
Manuscript ID:	draft
Manuscript Type:	Article
Date Submitted by the Author:	
Complete List of Authors:	Ogi, Hirotsugu; Osaka University, Graduate School of Engineering Science Okamoto, Ken; Osaka University Nagai, Hironao; Osaka University Fukunishi, Yuji; Osaka University Hirao, Masahiko; Osaka University

Replacement-Free Electrodeless QCM Using Nonspecific-Adsorption of Streptavidin on Quartz

Hirotsugu Ogi,*,†,‡ Ken Okamoto,† Hironao Nagai,† Yuji Fukunishi,† and Masahiko Hirao †

Graduate School of Engineering Science, Osaka University, Machikaneyama 1-3, Toyonaka, Osaka 560-8531, Japan

E-mail: ogi@me.es.osaka-u.ac.jp

Abstract

This paper proposes replacement-free and surface-modification-free quartz crystal microbalance (QCM) biosensor. Using significant nonspecific adsorption of streptavidin on naked quartz surfaces, target analyte is detected through biotin-tagged receptors on streptavidin. The wireless-electrodeless QCM technique is developed with a 30-μm-thick AT-cut quartz plate, whose fundamental resonance frequency is 55 MHz, and the naked quartz surfaces are used for the nonspecific adsorption of streptavidin. Once it is installed in the sensor cell, it can be used semipermanently; it never needs to be replaced. The affinity constant of streptavidin on quartz is determined to be 1.3×10^{-7}M. The flow rate affected the number of the adsorbed streptavidin on quartz as well as the binding velocity.

†Graduate School of Engineering Science
‡PRESTO, JST. 4-1-8 Honcho, Kawaguchi, Saitama, Japan

Introduction

Quartz-crystal microbalance (QCM) is a promising biosensor for evaluating interaction between biomolecules. Target molecules are adsorbed on receptors immobilized on quartz surface, increasing the effective mass to cause the decrease in the resonance frequency. Its sensitivity and usefulness are comparable with those of surface-plasmon-resonance biosensors,[1–3] which are also capable of monitoring binding reactions between proteins in real time. The sensitivity of a QCM biosensor is proportional to the square of the fundamental resonance frequency.[4] Conventional QCM biosensors use 5-10 MHz frequencies[1,5–8] and such a low-frequency measurement is affected by viscosity[9,10] and effective water mass[11–13] in addition to the added mass by the target protein. Simultaneous measurement of frequency and internal friction is proposed, making the measurement more quantitative.[11–18] Furusawa *et al.*[19,20] recently developed a 27-MHz QCM system to increase the sensitivity, although their method cannot adopt a flow-injection-analysis system.

Almost all sensor chips used in the existing biosensor systems need to be replaced because they use metallic thin films on their surfaces. We cannot use the same sensor chip for many times because washing with strong acid deteriorates the adhesion and metallic films fall off eventually. Biosensor chips must have been replaced, consuming cost and time. Therefore, a replacement-free biosensor has been desired.

We recently succeeded in developing a wireless-electrodeless high-frequency QCM (WE-QCM) by the antenna located outside the sensor cell.[21,22] It never needs electrodes on the quartz surfaces and can be the candidate of the replacement-free QCM. Also, avoiding heavy electrodes on the surfaces allows the high-frequency QCM because the large surface inertia due to the metallic electrodes do not participate in the resonator.[23] Indeed, our previous study reveals that a 500 nm electrode deteriorates the sensitivity by 40% in the case of the 55-MHz QCM.[24] The high-frequency QCM is also more quantitative because the viscosity effect becomes insignificant.[21,25,26]

In this study, we develop the replacement-free high-frequency WE-QCM. A 30-μm-thick AT-cut quartz plate is used, where the fundamental resonance frequency is near 55 MHz, much higher than the frequencies used in conventional QCM systems. First, we investigate the nonspecific-

binding ability of streptavidin by determining the affinity constant; we find significant nonspecific-adsorption behavior of streptavidin on the quartz surfaces compared with other proteins. This property can be used for the surface-modification-free biosensor. We then intend to detect human immunoglobulin G (hIgG) via the biotin-conjugated anti-human IgG antibody attached on streptavidin on quartz to evaluate the feasibility of the replacement-free biosensor.

Wireless-Electrodeless Measurement System

Figure 1 (a) shows the homebuilt sensor cell, where the 30-μm-thick AT-cut quartz plate with 3-mm diameter is located: A small part of the quartz oscillator is lightly sandwiched by 1-mm-thick silicon rubber sheets. (The gripping area is less than 3% of the whole area.) The flow channel is made inside the silicon rubbers so as to expose both surfaces of the oscillator to the flowing solution. The line antenna, consisting of two wires for generation and detection,[27,28] is embedded in the bottom Teflon block.

Figure 1(b) shows the electronics to measure the resonance frequency contactlessly by the line antenna. We develop the superheterodyne spectroscopy[29,30] with the intermediate frequency (ω_{IF}) of 150 MHz, which is provided by the local synthesizer. The master synthesizer generates a sinusoidal signal with the frequency of $\omega_{IF}+\omega_D$, where ω_D is the driving frequency and it is set to be close to the resonance frequency of the quartz oscillator ($\omega_D \sim 55$ MHz). The outputs from the two synthesizers enter the first multiplier and the driving-frequency signal with the frequency is produced by the following low-pass filter. After the high-power gated amplifier, the bust signal ($\sim$ 50 V_{pp} and 1-μs duration) is fed to the antenna wire for generation, which induces the electric field to cause pure-shear oscillation in the quartz crystal via the converse piezoelectric effect. After the excitation, the antenna wire for detection receives the reverberating signal of the oscillator vibration with the resonance frequency ω_R. This signal and the reference signal from the master synthesizer enter the second multiplier and the output signal is fed to the third multiplier after the bandpass filter set at ω_{IF}. The reference signal from the local synthesizer also enters the third multiplier, and

the output signal of the differential frequency component $\Delta\omega = \omega_R - \omega_D$ is extracted by the low-pass filter. This beating signal is integrated by the analog integrator, and the final output is stored in the personal computer to calculate the resonance frequency of the quartz oscillator ω_R. Our system allows the measurement of the resonance frequency every 3 ms with the fluctuation smaller than 10^{-6}. We made 500-times averaging for the stable measurement, so that the resonance frequency was obtained every 1.5 s with the frequency fluctuation of 1×10^{-7}. All electric components were obtained from RITEC Inc.

Experimental Procedure

The sensor cell is installed in the homebuilt flow-injection-analysis system as shown in Fig. 2. We select an analyte to be injected by the switching valve (FLOM Co., Ltd., Model 401) among eight vials. The carrier solution is a phosphate-buffer solution (PBS) with ph 7.4. A steady flow with the flow rate of 500 μL/min is supplied by the micropump (Uniflows Co. Ltd., Model 3005FSB2). The degasifier (Uniflows Co. Ltd., Model DG-7101) is located before the micropump to decrease the solvent gasses in the solution. After the micropump, the solution flows in a 3-m long Teflon tube column, which maintains the temperature of the solution at 37 °C. In the sensor cell, the solution flows along the both surfaces of the sensor chip as illustrated in Fig. 1(a). Note that a WE-QCM can use both surfaces as the sensing region.

First, we quantify the nonspecific-adsorption ability of streptavidin (SA), staphylococcus protein A (SPA), bovine serum albumin (BSA), human immunoglobulin G (hIgG), and hydroxy-end polyethylene glycol (Hydroxy-end PEG) on the naked quartz surface. The quartz oscillator is first cleaned by a piranha solution (98%H_2SO_4:33%H_2O_2=7:3) for 30 min and then rinsed by ultrapure water for 30 min and then by PBS for 1 h. The analyte solutions are injected and the resonance frequency change is recorded. The concentration of the injected proteins are varied between 10 and 100 μg/mL to determine equilibrium dissociation constant K_D and area density of the binding-site number σ_s^0.

Second, the multi-injection measurement is performed to evaluate the usefulness of streptavidin in the replacement-free QCM system. After the washing and rinsing procedure, a 100 μg/mL streptavidin/PBS solution is injected, which is followed by the injection of a 10 μg/mL biotin-conjugated anti-hIgG antibody/PBS solution. A 1 mg/mL biotin-conjugated PEG/PBS solution is then injected for blocking the remaining binding sites of streptavidin. hIgG solutions are then injected. The flow rate dependence on the binding behavior is also investigated.

Streptavidin was purchased from IBA Headquarters (product num. 2-0203-001; purity ∼95%). Biotin-conjugated anti-hIgG antibody (product num. 111-130-06) was from BioFX Laboratories, Inc. Biotin-conjugated PEG was from NANOCS INC. (product num.PEG5- 0001; molecular weight ∼5000). Hydroxy-end PEG (product num. PEG 6000 (33137); molecular weight ∼6000) was from Serva Electrophoresis. hIgG was from Athens Research and Technology, Inc. (product num. 16-16-090707; purity ∼95%). SPA was from Zymed Laboratories, Inc. (product num. 10-1100; purity ∼98%). BSA (No. 9048-46-8) was from Sigma-Aldrich Japan. All of other chemical substances were purchased from Wako Pure Chemical Industries Ltd.

Results

Figure 3 shows the typical frequency changes during the nonspecific adsorption of proteins on the quartz surfaces when a 100 μg/mL analyte solutions are injected. Significant frequency decrease occurs after the streptavidin solution arrives at the sensor cell. Figure 4 shows the equilibrium dissociation constant K_D and the number density of the total binding site of analyte on quartz in the nonspecific binding, σ_s^0. Streptavidin shows the smallest K_D value of 1.34×10^{-7}M, whereas it has a smaller σ_0 value. Figure 5 shows a frequency response during the multi-injection sequence for detecting hIgG. Figure 6 shows comparison of the binding behavior between two flow rates of 300 and 500 μg/mL. The higher flow rate causes faster binding reaction but deteriorates the total frequency change. Figure 7(a) shows binding curves between anti-hIgG antibody and hIgG solution with different concentrations. Figure 7(b) shows the plot between the exponential coefficient

of the binding curve and the analyte concentration.

Discussion

First, we emphasize that a real-time monitoring of nonspecific adsorption of proteins on α-SiO_2 surfaces will be only achieved by the WE-QCM system because other biosensor systems require metallic films on their sensor chip surfaces. Thus, this is the first time to quantify the significant adsorption of streptavidin on quartz. Furthermore, the WE-QCM has two important advantages over conventional QCMs with metallic films. (i) The WE-QCM can use almost whole sensor area on both surfaces because of the electrodeless nature. Only a few percent are is inactive due to the gripping by the silicon rubbers. On the other hand, conventional QCMs use only a single side and require metallic coatings near the center of the surfaces. Therefore, the outside area must remain uncoated to avoid the short-circuiting, and a large part of the sensor surfaces remain inactive. (ii)The WE-QCM is free from the deterioration of the sensitivity caused by the heavy metallic films as described above.

We discount the influence of the viscosity on the frequency change because of much higher fundamental frequency ($\sim$55 MHz) of our WE-QCM: The frequency change caused by the addition of the mass, Δf_m, and that by the viscosity change at the sensor surface, Δf_v, are given by [4,9,10]

$$\Delta f_m = 2N\frac{(\Delta m/A_e)}{\sqrt{\mu_q \rho_q}}\frac{A_e}{A_q}\cdot f_1^2 \tag{1}$$

$$\Delta f_v = \sqrt{N}\frac{\Delta\left(\sqrt{\rho_f \eta_f}\right)}{\sqrt{\pi \rho_q \mu_q}}\cdot f_1^{\frac{3}{2}}. \tag{2}$$

Here, integer N denotes the overtone number, f_1 the fundamental resonance frequency, and Δm the mass adsorbed on the sensor surfaces. A_e and A_q are the effective sensing area and the area of the crystal surface, respectively, and their ratio A_e/A_q is smaller than 1 for a conventional QCM using a single side of a quartz plate, but it nearly equals 2 for the WE-QCM. ρ_q and μ_q are the

mass density and the shear modulus of the crystal, and ρ_f and η_f are effective mass density and viscosity caused by the interaction between the surrounding liquid and the adsorbed film layer. The total frequency change is given by $\Delta f = \Delta f_m + \Delta f_v$. Thus, these equations indicate that the viscosity effect becomes insignificant compared with the mass-loading effect as the QCM frequency increases. For example, Zhou *et al.*[17] monitored binding reaction of hIgG on a hydrophobized sensor surface using a conventional 5 MHz QCM and they showed that $\Delta f/N$ was independent of N when the concentration of hIgG was lower than 115 μg/mL (770 nM). (Beyond this concentration, $\Delta f/N$ depended on N.) Equations (1) and (2) show that $\Delta f_m/N$ is independent of N and $\Delta f_v/N$ is inversely proportional to $\sqrt{N}$. Therefore, the viscosity effect is insignificant when the protein concentration is lower. Besides, our WE-QCM uses much higher frequency than the conventional QCM, further deteriorating the viscosity effect.

Next, we evaluate the kinetics in the nonspecific adsorption. Figure 3 highly indicates the high affinity of streptavidin on the quartz surfaces. Assuming that the adsorption kinetics obeys the pseudo-first-order law, the binding-site number σ_s per unit area on the quartz surfaces changes during the binding reaction[6,31]

$$\sigma_s = \frac{k_a C_A}{k_a C_A + k_d}\sigma_s^0 \left[1 - \mathrm{e}^{-(k_a C_A + k_d)t}\right] \tag{3}$$

Here, k_a and k_d denote association-rate and dissociation-rate constants, respectively. σ_s^0 denotes the total number density of the binding sites on quartz for corresponding protein. C_A is the concentration of the protein injected. The adsorbed mass is expressed by $\Delta m = A_e \sigma_s p_A / N_A$ with the molecular weight p_A and the Avogadro constant N_A. Taking A_e/A_q=2, $\Delta f = \Delta f_m$, and N=1, we have

$$\Delta f = -\frac{4 f_1^2}{\sqrt{\rho_q \mu_q}} \frac{p_A}{N_A} \sigma_s \tag{4}$$

σ_s^0 is then obtained by

$$\sigma_s^0 = \frac{\sqrt{\rho_q \mu_q}}{4 f_1^2} \frac{N_A}{p_A C_A k_a} \left(\frac{d\Delta f}{dt}\right)_{t=0} \tag{5}$$

We determined the slope $(d\Delta f/dt)_{t=0}$ at the beginning of the reaction (t=0) to deduce σ_s^0.

The resonance frequency changes exponentially with the exponential coefficient α(eqs. (3) and (4))

$$\alpha = k_a C_A + k_d, \tag{6}$$

yielding the kinetics constants k_a, k_d, and the equilibrium dissociation constant $K_D = k_d/k_a$ by plotting C_A versus α.[24] We thus determined K_D and σ_s^0, which are shown in Fig. 4.

Reproducibility of the measurement was not so great and the determined kinetics constants involved larger errors (∼10-40%) as shown in Fig. 4 than those determined for pairs with much higher affinity such as antigen-antibody reactions.[22,24] This will be caused by the difficulty of producing the same surface condition on the naked quartz crystal after the washing-rinsing procedure. Before the resonance frequency became stable enough, we had to wait about 30 min and the crystal surface would be deteriorated during the flow of the carrier solution. However, we can see significantly smaller K_D value of streptavidin compared with other materials. It is of the order of 10^{-7}M. Thus, streptavidin is a candidate base material for the replacement-free QCM. The binding site number between streptavidin and quartz is, however, the smallest, and the QCM sensitivity may be decreased for the detection of smaller molecules.

As shown in Fig. 5, we succeeded in detecting hIgG through the anti-hIgG antibody. Frequency changes caused by adsorption of streptavidin, biotin-conjugated anti-hIgG antibody, 6.7 nM hIgG, and 6 nM hIgG were 3664, 1748, 543, and 663 Hz, respectively. These values and eq. (1) evaluate amounts of adsorbed molecules to be 0.71, 0.12, 0.037, and 0.045 pmol, respectively. Streptavidin is a tetramer of the avidin unit and each unit binds one biotin molecule with extremely high affinity ($K_D \sim 10^{-15}$M). However, the number of anti-hIgG-antibody molecule adsorbed on streptavidin via the biotin label is only 17% of that of streptavidin. There are two possible reasons. Firstly, the steric hindrance of anti-hIgG antibody is marked due to its large molecular size. Then, it would be difficult to attach two or three anti-hIgG-antibody molecules onto one streptavidin molecule. Secondly, dissociation of streptavidin from the quartz surface occurred during the biotin-avidin binding reaction simultaneously. The flow rate in this study was 500 μL/min, much larger than the conventional flow injection system (∼50 μL/min). The flowing antibody molecules would

then peel the weakly bonded streptavidin off from the quartz surface via the avidin-biotin bond. Indeed, after the injection of the biotin-PEG, the frequency decreased for a while but increased gradually until the injection of hIgG solution, indicating peeling of streptavidin molecules. To investigate the flow-rate effect, we performed the similar measurement with a lower flow rate of 300 μL/min. The result is shown in Fig. 6(a). The ratio of the molecule number of adsorbed anti-hIgG antibody to that of streptavidin increased to be 64%, despite deterioration of the amount of adsorbed streptavidin on quartz (0.28 pmol). Also, the association velocity constant k_a appears to be decreased in all interactions. Our previous study revealed the significant dependence of apparent k_a and k_d values on the flow rate due to enhanced convection;[24] they decrease with the decrease in the flow rate, keeping the affinity value unchanged. Figure 6(b) compares binding curves with the two flow rates. The reaction velocity increases by the increase of the flow rate, but the total amount of the frequency change decreases because of the peeling behavior of streptavidin. Therefore, the flow rate is an important parameter in the replacement-free QCM with nonspecific adsorption of the base protein.

In Fig. 5, hIgG solutions are injected twice, causing totally 1206 Hz frequency change, or 0.082 pmol adsorption, which is about 70% of the amount of the anti-hIgG antibody adsorbed on streptavidin, indicating the high affinity between anti-hIgG antibody and hIgG. We deduced the affinity constant as shown in Fig. 7. The replacement-free QCM shows high enough sensitivity for clearly detecting hIgG at a concentration of 670 pM. The Langmuir plot in Fig. 7(b) yields the equilibrium dissociation constants of K_D=9.58 nM. We independently determined the affinity value using our previous wireless QCM method with self-assemble-monolayer base (10-carboxy-1-decanethiol) on Au,[22,24] which agreed with this value within 20% difference.

CONCLUSION

We developed a replacement-free wireless-electrodeless QCM system with 55 MHz fundamental frequency. The nonspecific adsorption of various proteins on the naked quartz surfaces was

evaluated quantitatively, and we reveal that streptavidin shows high affinity on quartz with $K_D = 1.34 \times 10^{-7}$M. Therefore, using streptavidin base on quartz, we can detect any analyte via biotin-conjugated receptors on streptavidin, where the sensor chip never needs to be replaced. Using biotin-conjugated anti-hIgG antibody, this system showed high enough sensitivity to detect a 670 pM hIgG solution. This system also works for determining the kinetics analysis.

The binding behavior is however affected by the flow rate. Higher flow rate accelerates biding reactions, but it causes peeling-off of the weakly-bonded streptavidin base from the quartz surfaces, deteriorating the detection sensitivity. This is a tradeoff between the measurement time and the sensitivity. Therefore, we need to select an appropriate flow rate in the use of the replacement-free QCM in the flow-injection analysis system.

Acknowledgement

A part of this study was supported by Life Phenomena and Measurement Analysis, PRESTO, by Japan Science and Technology Agency.

References

(1) Spangler, B. D.; Wilkinson, E. A.; Murphyb, J. T.; Tyler, B. J. Anal. Chim. Acta 2001, 444, 149-161.

(2) Laricchia-Robbio, L.; Revoltella, R. P. Biosens. Bioelectron. 2004, 19,1753-1758.

(3) Su, X.; Zhang, J. Sens. Actua. B 2004, 100, 309-314.

(4) Sauerbrey, G. Z. Phys. 1959, 155, 206-222.

(5) Muramatsu, H.; Dicks, M. D.; Tamiya, E.; Karube, I. Anal. Chem. 1987, 59, 2760-2763.

(6) LiuĄCY.; Yu, X.; Zhao, R.; Shangguan, D.; Bo, Z.; Liu, G. Biosens. Bioelectron. 2003, 19, 9-19.

(7) Kang, H.; Muramatsu, H. Biosens. Bioelectron. 2009, 24, 1318-1323.

(8) Edvardsson, M.; Svedhem, S.; Wang, G.; Richter, R.; Rodahl, M.; Kasemo, B. Anal. Chem. 2009, 81, 349-361.

(9) Kanazawa, K. K.; Gordon, J. G. Anal. Chim. Acta. 1985, 175, 99-105.

(10) Martin, S. J.; Granstaff, V. E.; Frye, G. C. Anal. Chem. 1991, 63, 2272-2281.

(11) Höök, F; Kasemo, B.; Nylander, T.; Fant, C.; Sott, K.; Elwing, H. Anal. Chem. 2001, 73, 5796-5804.

(12) Reimhult, E.; Larsson, C.; Kasemo, B.; Höök, F. Anal. Chem. 2004, 76, 7211-7220.

(13) Zong, Y.; Xu, F.; Su, X.; Knoll, W. Anal. Chem. 2008, 80, 5246-5250.

(14) Rodahl, M.; Höök, F.; Krozer, A.; Brzezinski, P.; Kasemoa, B. Rev. Sci. Instrum. 1995, 66, 3924-3930.

(15) Rodahl, M.; Kasemo, B. Sens. Actuat. 1996, 54, 448-456.

(16) Höök, F; Rodahl, M.; Brzezinski, P.; B. Kasemo, B. Langmuir 1998, 14, 729-734.

(17) Zhou, C.; Friedt, J. M.; Angelova, A.; Choi, K. H.; Laureyn, W.; Frederix, F.; Francis, L. A.; Campitelli, A.; Engelborghs, Y.; Borghs, G. Langmuir 2004, 20, 5870-5878.

(18) Jonsson, M. P.; Jönsson, P.; Höök, F. Anal. Chem. 2008, 80, 7988-7995.

(19) Furusawa, H.; Ozeki, T.; Morita, M.; Okahata, Y. Anal. Chem. 2009, in press (DOI: 10.1021/ac802412t).

(20) Furusawa, H.; Komatsu, M.; Okahata, Y. Anal. Chem. 2009, in press (DOI: 10.1021/ac8022229).

(21) Ogi, H.; Motohisa, K.; Matsumoto, T.; Hatanaka, K.; Hirao, M. Anal. Chem. 2006. 78, 6903-6909.

(22) Ogi, H.; Motohisa, M.; Hatanaka, K.; Ohmori, T.; Hirao, M.; Nishiyama, M. Biosens. Bioelectron. 2007, 22, 3238-3242.

(23) Ogi, H.; Ohmori, T.; Hatanaka, K.; Hirao, M.; Nishiyama, M. Jpn. J. Appl. Phys. 2008, 47, 4021-4023.

(24) Ogi, H.; Fukunishi, Y.; Omori, T.; Hatanaka, K.; Hirao, M.; Nishiyama, M. Anal. Chem. 2008, 80, 5494-5500.

(25) Ogi, H.; Hatanaka, K.; Fukunishi, Y.; Nagai, H; Hirao, M.; Nishiyama, M. Jpn. J. Appl. Phys. 2009, in press.

(26) Ogi, H.; Fukunishi, Y.; Nagai, H.; Okamoto, K.; Hirao, M.; Nishiyama, M. Biosen. Bioelectron. 2009, submitted.

(27) Ogi, H.; Niho, H.; Hirao, M. Appl. Phys. Lett. 2006, 88, 141110.

(28) Ogi, H.; Inoue, T.; Nagai, H.; Hirao, M. Rev. Sci. Instrum. 2008, 79, 053701.

(29) Hirao, M.; Ogi, H.; Fukuoka, H. Rev. Sci. Instrum. 1993, 64, 3198-3205.

(30) Petersen, G. L.; Chick, B. B.; Fortunko, C. M.; Mirao, M. Rev. Sci. Instrum. 1994, 65, 192-198.

(31) Eddowes, M. J. Biosensors 1987, 3, 1-15.

Figure Caption

Fig. 1 (a) Homebuilt sensor cell consisting of the line antenna, two Teflon covers, and two silicon rubbers (1 mm) sandwiching the 30-μm-thick quartz plate. Upper and lower figures show top view and side view, respectively. Solutions flow in the shaded area. (b) Signal flow for measuring the resonance frequency of the quartz oscillator with the noncontacting manner.

Fig. 2 Homebuilt flow-injection-analysis system. The sensor cell is installed in the temperature control room where the temperature is kept at 37 °C

Fig. 3 Frequency changes observed for injection of 100-μg/mL-concentration proteins in PBS; PEG, SPA, BSA, hIgG, and streptavidin.

Fig. 4 The equilibrium dissociation constant K_D and the total number density of the binding sites σ_s^0 for nonspecific adsorption of various proteins on quartz surfaces.

Fig. 5 A frequency change observed in a multi-injection measurement. The flow rate is 500 μL/min.

Fig. 6 (a)A frequency response in a multi-injection measurement for a flow rate of 300 μL/min. (b) Comparison of binding curves for streptavidin on quartz (SA), anti-hIgG antibody on streptavidin (anti-hIgG), and hIgG on anti-hIgG antibody (hIgG) between two flow rates of 500 (open marks) and 300 (solid marks) μL/min.

Fig. 7 (a) Frequency changes with different concentrations of hIgG solutions observed at a flow rate of 500 μL/min. Broken lines are fitted theoretical function (eq. (4)). (b) The relation-

ship between the exponential coefficient α versus the concentration of hIgG. The slope and intercept yield the kinetics constants.

References

.

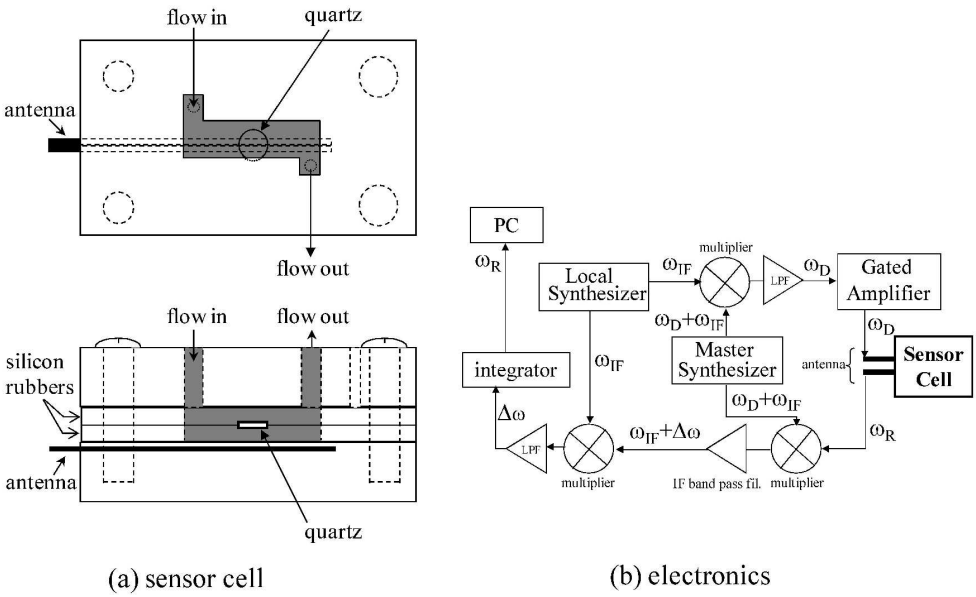

(a) sensor cell (b) electronics

227x138mm (600 x 600 DPI)

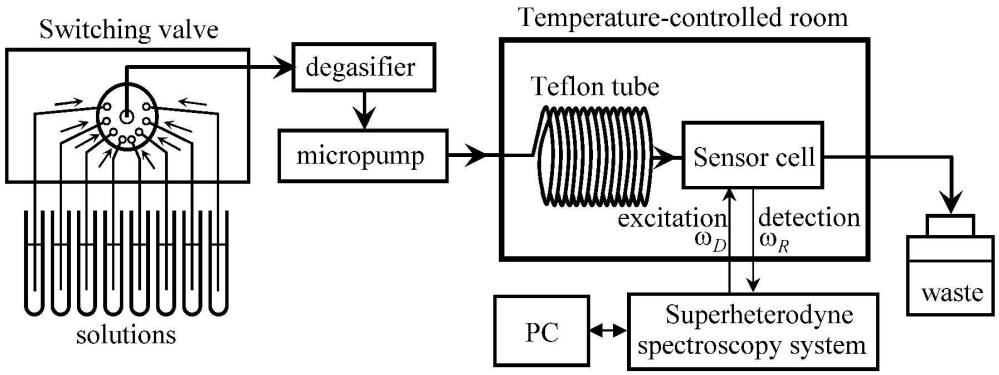

151x58mm (600 x 600 DPI)

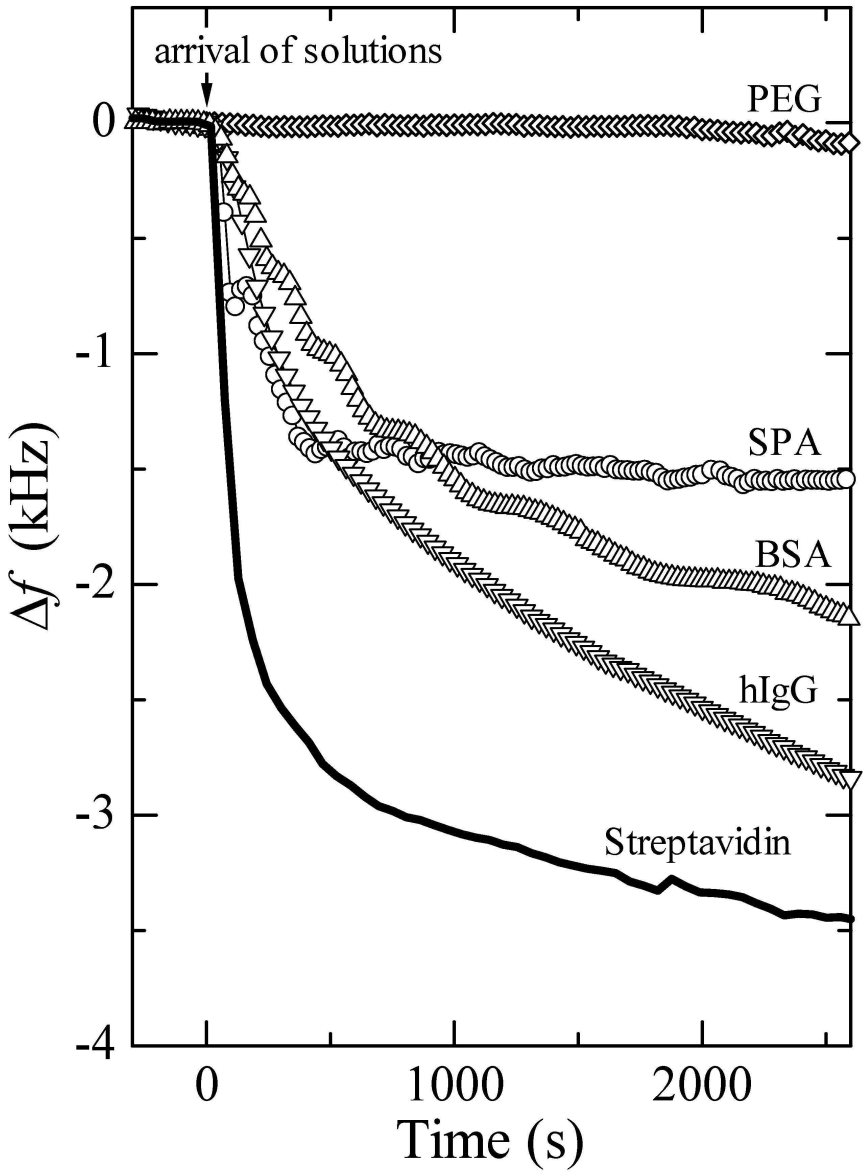

111x150mm (600 x 600 DPI)

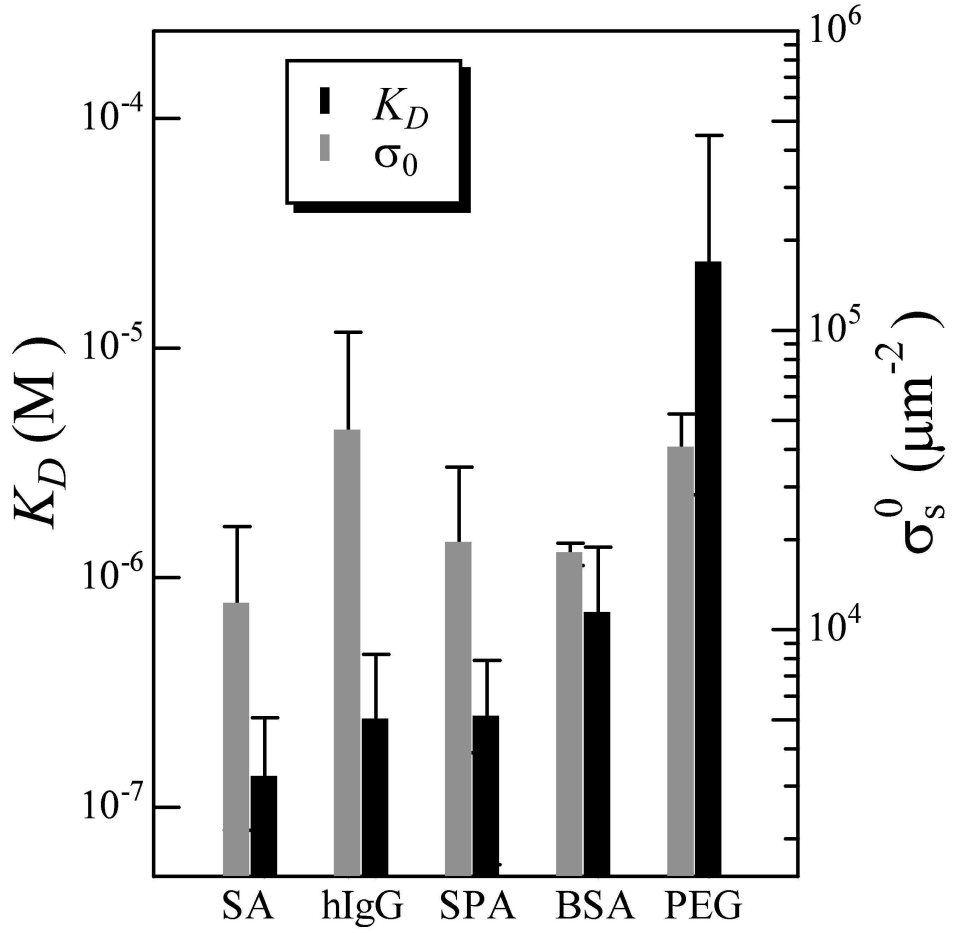

119x113mm (600 x 600 DPI)

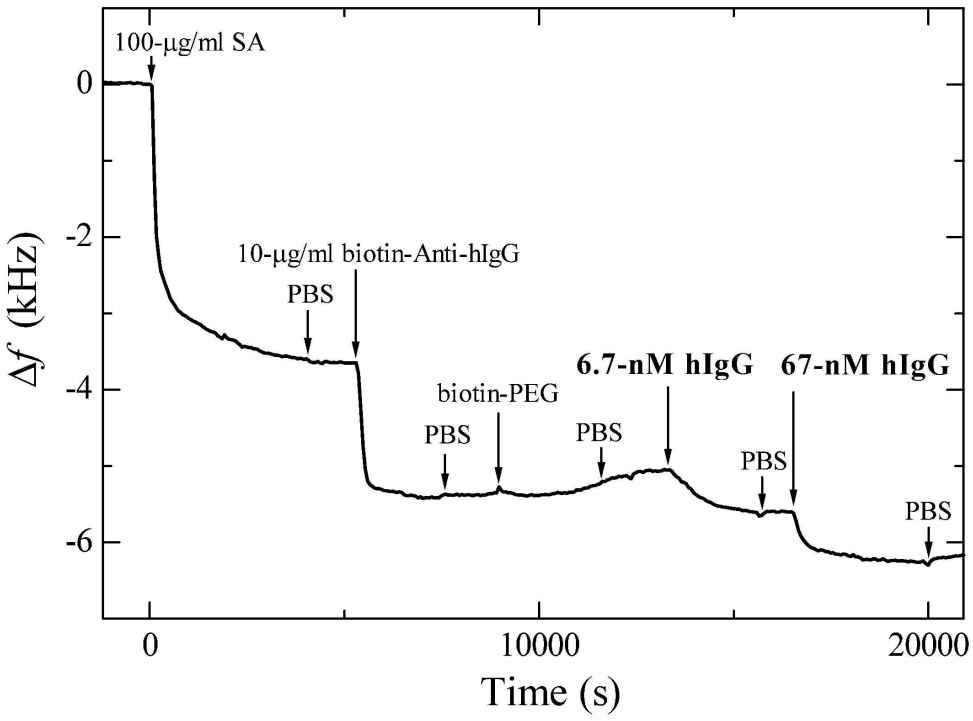

185x135mm (600 x 600 DPI)

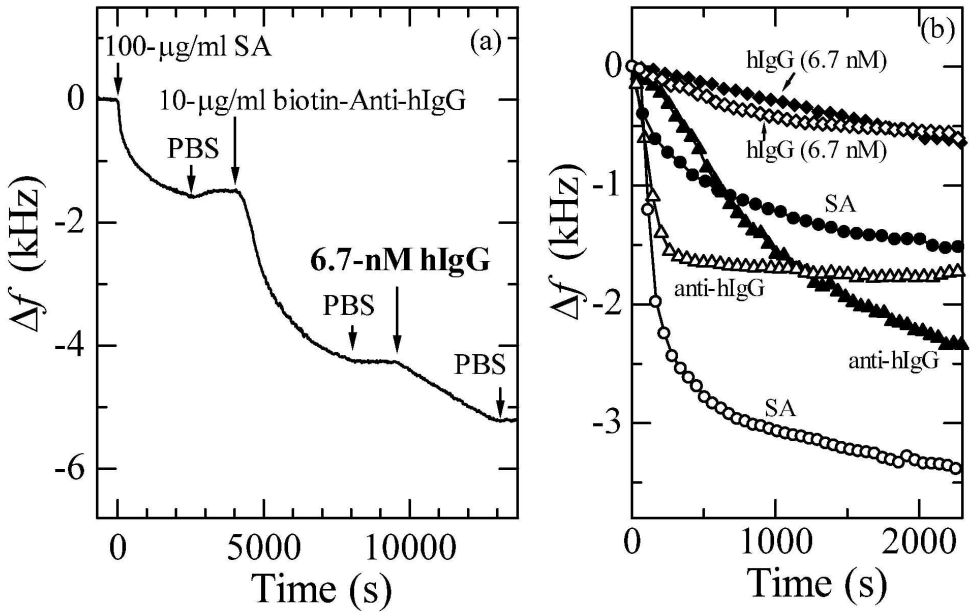

166x105mm (600 x 600 DPI)

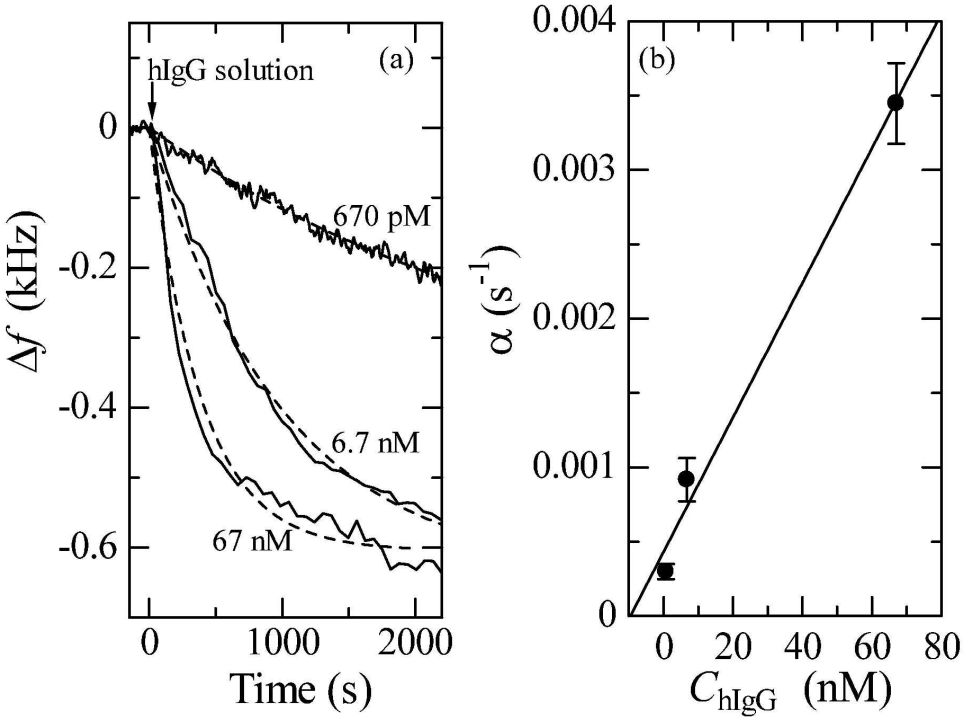

160x117mm (600 x 600 DPI)